ELSEVIER

Journal of Quantitative Spectroscopy & Radiative Transfer 95 (2005) 21–32

Journal of Quantitative Spectroscopy & Radiative Transfer

www.elsevier.com/locate/jqsrt

A semi-analytic technique to speed up successive order of scattering model for optically thick media

Minzheng Duan*, Qilong Min

Atmospheric Sciences Research Center, State University of New York, 251 Fuller Road, Albany, NY 12203, USA

Received 19 May 2004; accepted 2 September 2004

Abstract

A semi-analytic technique has been developed to speed up the integration of radiative transfer over optically thick media for the successive order of scattering (SOS) method. Based on the characteristics of the internal distribution of scattering intensity, this technique uses piecewise analytic eigenfunctions to fit internal scattering intensities and integrates them analytically over optical depth. This semi-analytic approach greatly reduces the number of sub-layers required for accurate radiative transfer calculation based on the SOS method. Results show that an accuracy of 1% for both flux and radiance (polar angle less than 67°) can be achieved with a significantly small number of layers. This technique is accurate and efficient and makes the SOS method applicable for optically thick scattering media.

Keywords: Radiative transfer; Scattering; Cloud

1. Introduction

The successive order of scattering (SOS) method is physically straightforward by computing contributions of each scattering event. Since the SOS method traces photons for each scattering event, the inhomogeneous structure of a medium as well as gaseous absorption process can be

*Corresponding author. Tel.: +1 518 437 8791; fax: +1 518 437 8758.
E-mail addresses: dmz@asrc.cestm.albany.edu (M. Duan), min@asrc.cestm.albany.edu (Q. Min).

0022-4073/$ - see front matter
doi:10.1016/j.jqsrt.2004.09.027

incorporated in the calculation in terms of integration along the photon path [1]. It has potentials for parameterization of radiative transfer in remote sensing and global climate modeling. However, substantial computational burden due to a slow convergence with a high single scattering albedo and a large number of sub-layers for an optically thick medium, prevents extensive uses of the SOS method. To improve computational efficiency and accuracy of the SOS method, several techniques have been proposed to simplify the integration of the source function along photon paths, such as a polynomial fit [2] and a linear-exponent fit [1]. Both methods significantly reduce the computational time with a smaller number of sub-layers and an easier analytical integration. However, these methods still require a substantial number of sub-layers for optically thick media. In this paper, we develop a semi-analytic approach to further reduce the computational time so that the SOS can be applied to optically thick media. A detailed description of the method is given in Section 2, and extensive validations will be discussed in Section 3.

2. The SOS method and issues

The solution of radiative transfer for the SOS method is expressed as a summation of contributions of all successive orders of scattering [1,3]:

$$I(\tau,\mu,\phi)=\sum_{n=1}^{\infty} I_n(\tau,\mu,\phi), \tag{1}$$

where I is the intensity at optical depth τ, cosine of polar angle μ, and azimuthal angle ϕ; subscript n stands for the nth scattering order. Since the integration is separated for each azimuthal direction, we eliminate ϕ in the following discussion. For each scattering order, the downward and upward intensities, $I_n^{\downarrow}$ and $I_n^{\uparrow}$, can be given by integrations along optical paths

$$I_n^{\uparrow}(\tau,\mu)=I_n^{\uparrow}(\tau_*,\mu)\exp\{-(\tau_*-\tau)/\mu\}+\int_{\tau}^{\tau_*} J_n(t,\mu)\exp\{-(t-\tau)/\mu\}\,\mathrm{d}t/\mu,$$

$$I_n^{\downarrow}(\tau,\mu)=I_n^{\downarrow}(\tau_0,\mu)\exp\{-(\tau-\tau_0)/\mu\}+\int_{\tau_0}^{\tau} J_n(t,\mu)\exp\{-(\tau-t)/\mu\}\,\mathrm{d}t/\mu, \tag{2}$$

where J_n is the source function for the nth scattering order, τ_0 and τ_* are the upper and bottom boundary layers, respectively. The source function, J_n, can be written as

$$J_1=\frac{\omega}{4\pi}\exp(-\tau/\mu_0)P(\tau,\mu;\mu_0)F_0,$$

$$J_n=\frac{\omega}{4}\int_{-1}^{1} P(\tau,\mu;\mu')I_{n-1}(\tau,\mu')\,\mathrm{d}\mu' \quad n\geqslant 2, \tag{3}$$

where F_0 is the extra-terrestrial solar irradiance, μ_0 is the cosine of solar zenith angle, P is the scattering phase function. The intensity of the first scattering order, I_1, can be solved analytically as

$$I_1^{\uparrow}(\tau,\mu)=I_1^{\uparrow}(\tau_*,\mu)\exp\{-(\tau_*-\tau)/\mu\}+\frac{\omega}{4\pi}\frac{\mu_0 P(\tau,\mu;\mu_0)F_0}{\mu_0+\mu}(\mathrm{e}^{-\tau/\mu_0}-\mathrm{e}^{-\tau_*/\mu_0}\mathrm{e}^{-(\tau_*-\tau)/\mu}),$$

$$I_1^{\downarrow}(\tau,\mu) = I_1^{\downarrow}(\tau_0,\mu)\exp\{-(\tau-\tau_0)/\mu\} + \frac{\omega}{4\pi}\frac{\mu_0 P(\tau,-\mu;\mu_0)F_0}{\mu_0-\mu}(e^{-\tau/\mu_0} - e^{-\tau_0/\mu_0}e^{-(\tau-\tau_0)/\mu}). \quad (4)$$

For higher scattering orders, the distribution of J_n inside a layer is more complicated and does not have a simple analytic expression. The intensity, however, has to be integrated numerically. To ensure numerical integration accuracy, an optically thick layer is traditionally divided into multiple sub-layers with a small incremental optical depth (<0.05). Therefore, the distribution of the source function within a sub-layer can be assumed to be linear. A layer with optical depth of 5 has to be sliced into at least 200 sub-layers to achieve an accuracy of 1%. Furthermore, Eq. (1) converges very slowly when the single scattering albedo approaches 1 for an optical thick media. For example, several hundreds of successive scattering are necessary for optical depth greater than 5.

2.1. Semi-analytical approach for integration

Herman et al. [2] extensively studied internal distributions of source function in the Gauss–Seidel method and noted that rapid changes of intensity occur near layer boundaries. They divided a layer into unevenly spaced sub-layers with an incremental optical depth from both boundaries to the layer center. Further, they fitted the source function into a polynomial function and integrated it analytically. For a case of optical depth of 5, Herman et al.'s method requires 52 sub-layers to get a satisfactory result. Recently, Min and Duan [1] used a linear-exponent function to fit the internal source function of a sub-layer. For evenly spaced slices, a layer of optical depth of 5 requires 50 sub-layers for a layer of optical depth of 5. If an unevenly spaced scheme is adopted, the number of sub-layers may be reduced slightly. However, both approaches are still inadequate for dealing with cases with optical depth larger than 5.

Based on the discrete ordinate method, the intensity distribution in a homogeneous layer can be expressed as

$$I(\tau,\mu) = \sum_{k=1}^{K} B_k^- X_k^-(\mu)e^{\lambda_k\tau} + \sum_{k=1}^{K} B_k^+ X_k^+(\mu)e^{-\lambda_k\tau} + C(\mu)e^{-\tau/\mu_0}, \quad (5)$$

where $X_k^{\pm}(\mu)$ are the eigenvectors relative to eigenvalues of $\pm\lambda_k$, which depend upon the single scattering properties of the scattering layer [4]. $B_k^{\pm}$ and C are coefficients determined by boundary conditions. Eq. (5) illustrates the characteristics of the internal distribution of intensity within a layer and provides an analytical formula of internal distribution of intensity for all orders of successive scattering. Considering numerical implementation, we select a two-stream approximation with an unevenly spaced piecewise fitting. Fig. 1 illustrates the coordinates of this semi-analytical piecewise fitting and its corresponding indexes. The analytic function for each sub-piece can be written as

$$I_{n-1}(\tau,\mu) = X_m^-(\mu)e^{\lambda\tau} + X_m^+(\mu)e^{-\lambda\tau} + Y_m(\mu)e^{-\tau/\mu_0} \quad \tau\in(\tau_{2m-2},\tau_{2m}). \quad (6)$$

To ensure the computational stability, the coefficients in the above equation are scaled by

$$B_m^-(\mu) = X_m^-(\mu)e^{\lambda\tau_{2m}},$$

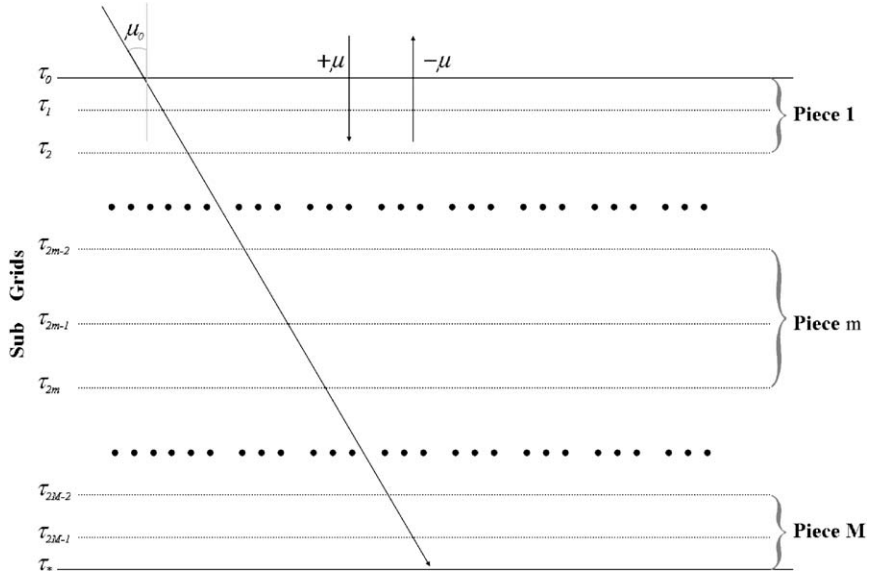

Fig. 1. Coordination of the SOS method.

$$B_m^+(\mu) = X_m^+(\mu)\mathrm{e}^{-\lambda\tau_{2m-2}},$$

$$C_m(\mu) = Y_m(\mu)\mathrm{e}^{-\tau_{2m-2}/\mu_0}. \tag{7}$$

Inserting Eq. (7) into Eq. (6), we have a numerically stable equation

$$I_{n-1}(\tau,\mu) = B_m^-(\mu)\mathrm{e}^{-\lambda(\tau_{2m}-\tau)} + B_m^+(\mu)\mathrm{e}^{-\lambda(\tau-\tau_{2m-2})} + C_m(\mu)\mathrm{e}^{-(\tau-\tau_{2m-2})/\mu_0}, \quad \tau\in(\tau_{2m-2},\tau_{2m}), \tag{8}$$

while the coefficients of B_m^+, B_m^-, C_m, and λ can be given by nonlinearly fitting I_{n-1} as a function of optical depth within (τ_{2m-2},τ_{2m}) for each direction. Inserting Eq. (8) into Eq. (3), the source function J_n for the nth scattering order can be given as

$$J_n(\tau,\mu) = \Re_m^-(\mu)\mathrm{e}^{-\lambda(\tau_{2m}-\tau)} + \Re_m^+(\mu)\mathrm{e}^{-\lambda(\tau-\tau_{2m-2})} + z_m(\mu)\mathrm{e}^{-(\tau-\tau_{2m-2})/\mu_0}, \quad \tau\in(\tau_{2m-2},\tau_{2m}), \tag{9}$$

where $\Re_m^+, \Re_m^-, z_m$ can be easily given by Eqs. (3) and (8). Inserting Eq. (9) into Eq. (2), the final solution can be integrated analytically as

$$I_n^{\downarrow}(\tau_j,\mu) = I_n^{\downarrow}(\tau_{2m-2},\mu)\mathrm{e}^{-\delta\tau/\mu} + \frac{\Re_m^-(\mu)}{1+\lambda\mu}[\mathrm{e}^{-\lambda\varepsilon\tau} - \mathrm{e}^{-\lambda\Delta\tau}\mathrm{e}^{-\delta\tau/\mu}]$$
$$+ \frac{\Re_m^+(\mu)}{1-\lambda\mu}[\mathrm{e}^{-\lambda\delta\tau} - \mathrm{e}^{-\delta\tau/\mu}] + \frac{\not{c}_m(\mu)\mu_0}{\mu_0-\mu}[\mathrm{e}^{-\delta\tau/\mu_0} - \mathrm{e}^{-\delta\tau/\mu}] \quad j = 2m-1, 2m, \tag{10a}$$

$$I_n^{\uparrow}(\tau_j,\mu) = I_n^{\uparrow}(\tau_{2m},\mu)\mathrm{e}^{-\varepsilon\tau/\mu} + \frac{\Re_m^-(-\mu)}{1-\lambda\mu}[\mathrm{e}^{-\lambda\varepsilon\tau} - \mathrm{e}^{-\varepsilon\tau/\mu}]\frac{1}{2} + \frac{\Re_m^+(-\mu)}{1+\lambda\mu}[\mathrm{e}^{-\lambda\delta\tau} - \mathrm{e}^{-\lambda\Delta\tau}\mathrm{e}^{-\varepsilon\tau/\mu}]$$
$$+ \frac{z_m(-\mu)\mu_0}{\mu_0+\mu}[\mathrm{e}^{-\delta\tau/\mu_0} - \mathrm{e}^{-\Delta\tau/\mu_0}\mathrm{e}^{-\varepsilon\tau/\mu}] \quad j = 2m-2, 2m-1, \tag{10b}$$

where $\delta\tau = \tau_j - \tau_{2m-2}$; $\varepsilon\tau = \tau_{2m} - \tau_j$; $\Delta\tau = \tau_{2m} - \tau_{2m-2}$. Such a piecewise and semi-analytical approach will ensure computational efficiency and accuracy.

2.1.1. Selection of λ

For further simplicity, we prescribe the eigenvalue, λ, based on the single scattering properties of the layer at a particular scattering order. Thus, Eq. (8) becomes explicitly a linear equation, and coefficients, B_m^+, B_m^-, C_m, can be solved analytically and efficiently from intensities at 3 sub-layers at τ_{2m-2}, τ_{2m-1} and τ_{2m}, as illustrated in Fig. 1. As shown in Figs. 2 and 3, the internal distribution of intensity varies gradually and systematically as the scattering order increases due to radiation smoothing of multiple scattering. Such internal variation is characterized by the eigenvalues of the radiation field for a particular scattering order. The eigenvalue decreases as the scattering order increases. Therefore, we assume that the eigenvalue at the nth scattering order, λ_n, changes in the following way:

$$\lambda_n = \alpha\lambda_{n-1} = \alpha^{n-1}\lambda_1,$$

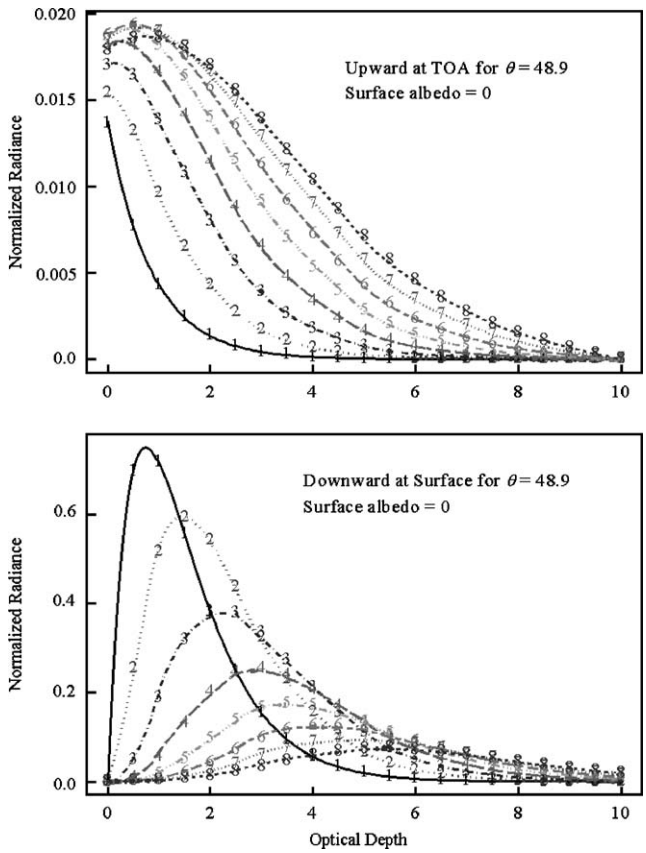

Fig. 2. Intensity distribution along optical depth of each scattering. The upper and lower panel are for upward at TOA and downward radiance at surface, respectively. Results in this figure are for polar angle 48.9, optical depth of 10, single scattering albedo of 0.99 and surface albedo of 0.0.

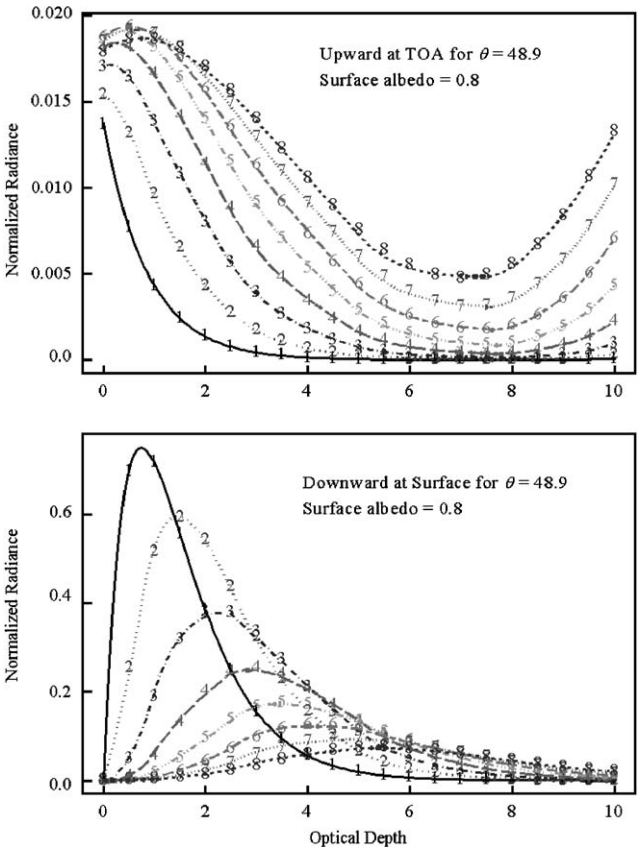

Fig. 3. Same as Fig. 2 except for surface albedo of 0.8.

where n is the scattering order, and α is the reduction multiplier. Since we will divide an entire homogeneous layer into unevenly spaced slices and fit each piece (3 sub-layers) with Eq. (8), the slow variations are captured by the piecewise fitting process and the fast variations are determined by the two-stream analytical fitting. Therefore, we assume that λ_1 is a fraction (80%) of the larger eigenvalue of a four-stream approximation, which is determined by the single scattering properties of the homogeneous layer. Based on trial and error, the multiplier is set to be 0.65.

2.1.2. *Unevenly spaced sub-layers*

Figs. 2 and 3 also illustrate that rapid changes of internal intensity for all scattering orders occur near the top and bottom of the layer. In order to simulate the rapid changes near layer boundaries accurately, an unevenly spaced grid scheme is adopted. We use a quadratic function to define the unevenly spaced sub-layer from the layer boundary to the layer center as

$$\tau_i = 0.1 + 0.14i + ci^2 \quad \text{for } \tau \geqslant 1,$$

$$\tau_i = 0.05(1. + i + ci^2) \quad \text{for } \tau < 1,$$

where the coefficient c is determined by the total number of sub-layers, $N = 2N_{1/2} - 1$. For a given optical depth of a layer, τ, the total value $N_{1/2}$ and c, can be expressed as

$$N_{1/2} = \mathrm{INT}\left(2.4 + \sqrt{\tau}/2 + \tau/4\right),$$

$$c = (\tau - 0.2 - 0.28N_{1/2})/2N_{1/2}^2 \quad \text{for } \tau \geqslant 1,$$

$$c = (10\tau - 1 - N_{1/2})/N_{1/2}^2 \quad \text{for } \tau < 1.$$

In this scheme, the optical depth of the sub-layer increases from the top and bottom of the layer to the layer center. For layers with optical depths of 5, 10, 20 or 50, the unevenly spaced scheme only requires 7, 11, 17 or 35 sub-layers, respectively, substantially reducing the number of sub-layers for a thick media. For example, for an optical depth of 5, the number of sub-layers for the simple linear scheme, the polynomial fitting scheme, and the linear-exponent fitting scheme are 152, 52 and 50, respectively.

2.2. Convergence of successive scattering

The solution convergence of the SOS method becomes very slow when the single scattering albedo of an optically thick layer tends to 1. It is necessary to accelerate the convergence to reduce the computational burden of the SOS method. Lenoble [3] noticed that for conservative scattering of an optically thick media, the ratio of two successive scattering radiances asymptotically approaches a constant. Fig. 4 shows ratios of I_n/I_{n-1} as a function of scattering order at different levels for a case with total optical depth of 10. In this simulation, we set the single scattering albedo to 0.99999 and the surface albedo to 0.0. The upper panel is for upward radiances for a polar angle of 48.9° and the lower panel for downward radiances at the same polar angle. It is clear that when the scattering order exceeds 40, the ratio of the two successive scattering radiances approaches 0.93 at all levels. The same holds true at other polar angles, as shown in Fig. 5. The fundamental reason is that photons lose the memory of their origin after several scattering events and thus the radiation field asymptotically reaches a diffusion equilibrium state. This provides a further way to accelerate the convergence, i.e., the summation of Eq. (1) can be truncated at the nth order of scattering when the ratio approaches a constant. The reminder can be replaced by a geometric series as

$$I(\tau, \mu, \phi) = \sum_{n=1}^{N-1} I_n(\tau, \mu, \phi) + I_N(\tau, \mu, \phi)/(1 - b), \tag{10}$$

where $b = I_N/I_{N-1}$. Therefore, we significantly reduce computational time without calculating higher order of scattering.

3. Results

An extensive sensitivity study has been conducted to test the efficiency and accuracy of this semi-analytical approach. Those tests are aimed at two kinds of potential applications of the SOS

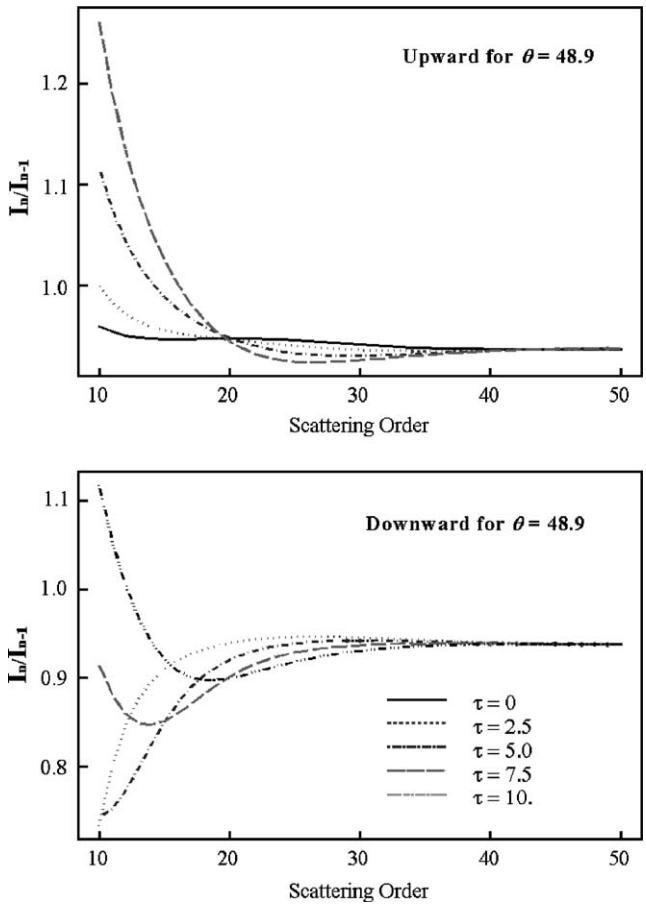

Fig. 4. Ratio of I_n/I_{n-1} as a function of scattering order at different optical depths. The upper and lower panel are for upward and downward radiance, respectively; polar angle is 48.9, $\omega = 0.99$, surface albedo is 0.0, total optical depth is 10.

method: intensity and flux. Based on current accuracies of most remote sensing instruments and models, we set the goal of accuracy of this approach to be better than 1% for both calculations. We used DISORT as our benchmark model to compute the total radiances at the top and bottom of the atmosphere [5]. For each scattering order, we computed the benchmark results of intensity distributions using the SOS method with a small incremental optical depth of 0.025.

Fig. 2 shows the comparison of internal intensity distributions between benchmark results and semi-analytical calculations with 11 sub-layers for total optical depth of 10. In this case, the single scattering albedo is 0.99 and the surface albedo is 0.0. The numbers in Fig. 2 represent the benchmark values for the corresponding scattering orders. The lines indicate the results of this semi-analytical method and illustrate that the piecewise eigenfunction fitting approach can simulate the internal distributions of intensity well for each scattering order. Fig. 3 shows a case with the same settings as Fig. 2 except for a surface albedo of 0.8. It further illustrates that

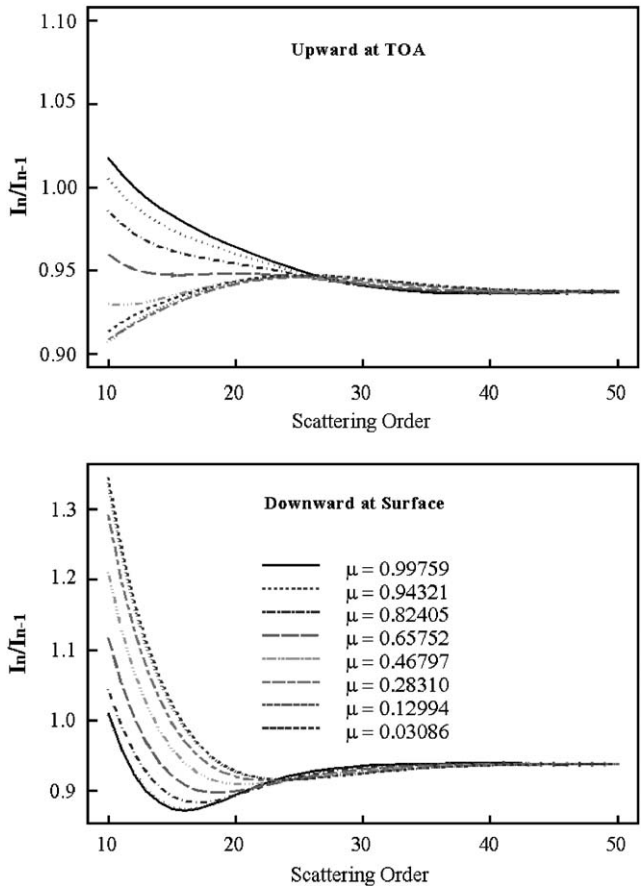

Fig. 5. Ratios of I_n/I_{n-1} as a function of scattering order at different polar angles. The upper and lower panel are for upward at TOA and downward radiance at surface, respectively; $\omega = 0.99$, surface albedo is 0.0, total optical depth is 10.

unevenly spaced piecewise eigenfunction fitting produces accurate internal distribution of intensity near both layer boundaries.

Fig. 6 shows the comparison of intensity at the top and bottom of the atmosphere as a function of polar angles for four different cases with total optical depths of 5, 10, 20 and 50. The left panels are for upward radiances and their differences at TOA while the right panels are for downward values at the bottom of atmosphere. The benchmark results are calculated from DISORT. It shows that the relative errors are less than 1% when the polar angles are smaller than 67°. For large polar angles ($>67°$), the errors are about a few percent. However, intensities at large polar angles contribute very little to the total flux. As listed in Table 1, the accuracy of fluxes at the top and bottom of the atmosphere for this semi-analytical approach is better than 1%. In most applications, observations at extreme polar angles ($>67°$) are seldom used because a simple plane-parallel model is no longer applicable. Furthermore, it is possible to improve accuracy at large polar angles by slicing the layer based on slant

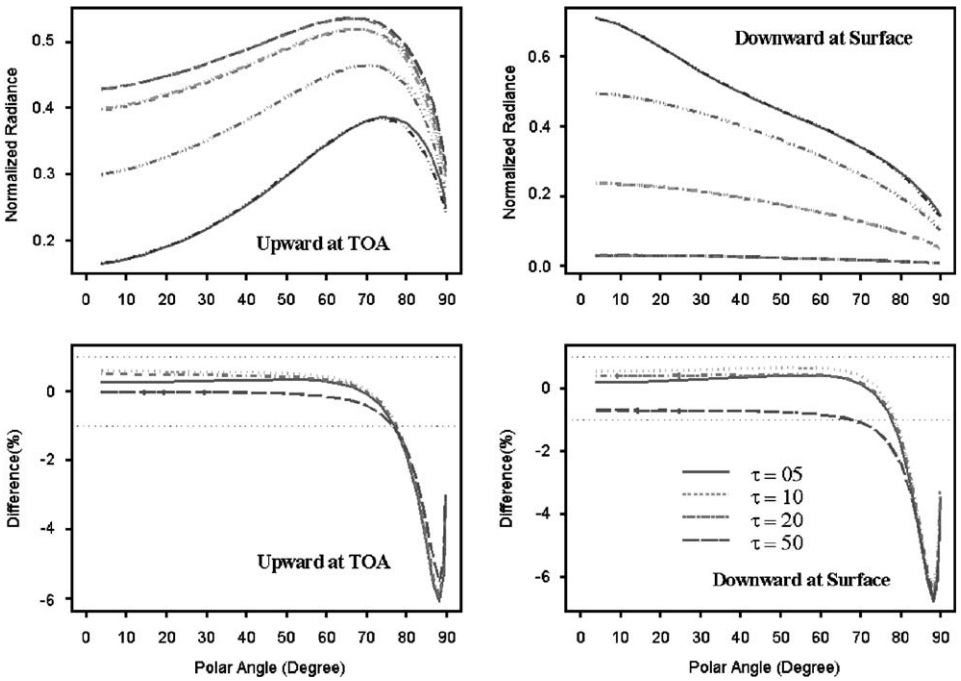

Fig. 6. Intensity and its difference distribution with polar angles. The left panels are for upward at TOA, the right panels for downward at bottom of atmosphere, $\omega = 0.99$, surface albedo is 0.0.

optical depth, i.e., different polar angles will space differently. Doing so would increase computational time a bit.

4. Summary

Two obstacles prevent extensive use of the SOS method: a large number of sub-layers and slow convergence for optically thick medium. In this paper, we exploited a piecewise analytic eigenfunction to fit the internal distribution of intensities for optically thick media. The piecewise eigenfunction approach substantially reduces the number of sub-layers required for accurately computing the radiative transfer via the SOS method. It requires only seven sub-layers for a conservative scattering case with an optical depth of 5, a seven-fold reduction in computational time compared to existing fast methods. For thicker optical layers, it reduces computational time even more dramatically. For example, 11, 17 and 35 sub-layers are sufficient for conservative scattering with optical depths of 10, 20 and 50, respectively. Furthermore, we truncate the calculation at the scattering order when the ratio of two successive scattering approaches a constant, and replace the higher order contributions with a geometric series. For a conservative scattering with a thick optical depth, this method needs only 40 successive scattering orders to achieve the required accuracy. More importantly, extensive case studies show an accuracy of 1% for both flux and radiance calculations (with polar angles less than 67°). This technique is accurate

Table 1
Upward flux at TOA and downward flux at bottom of atmosphere and comparison with that of DISORT

τ	$F^{\uparrow}_{\text{disort}}$	$F^{\uparrow}_{\text{sos}}$	Δ (%)	$F^{\downarrow}_{\text{disort}}$	$F^{\downarrow}_{\text{sos}}$	Δ (%)
For $\omega = 0.99$ *and* $A = 0.0$						
5	6.9893(−1)	6.9967(−1)	0.11	1.7738	1.7762	0.14
10	1.0509	1.0548	0.37	1.1794	1.1849	0.47
20	1.2892	1.2930	0.29	5.6552(−1)	5.6723(−1)	0.30
50	1.3644	1.3617	−0.20	7.2217(−2)	7.1605(−2)	−0.85
For $\omega = 0.99$ *and* $A = 0.8$						
5	1.8028	1.8036	0.04	2.4637	2.4671	0.14
10	1.5992	1.6045	0.33	1.8683	1.8766	0.44
20	1.4283	1.4320	0.26	9.8877(−1)	9.9122(−1)	0.25
50	1.3668	1.3640	−0.20	1.3053(−1)	1.2950(−1)	−0.79
For $\omega = 0.5$ *and* $A = 0.0$						
5	3.6086(−2)	3.5975(−2)	−0.31	8.9548(−2)	8.9237(−2)	−0.35
10	3.6112(−2)	3.6000(−2)	−0.31	3.2665(−3)	3.2521(−3)	−0.44
20	3.6112(−2)	3.6000(−2)	−0.31	4.1653(−6)	4.2048(−6)	0.95
50	3.6112(−2)	3.5995(−2)	−0.32	1.0014(−14)	1.0428(−14)	4.13
For $\omega = 0.5$ *and* $A = 0.8$						
5	3.7907(−2)	3.7802(−2)	−0.28	9.1717(−2)	9.1523(−2)	−0.21
10	3.6114(−2)	3.6002(−2)	−0.31	3.3394(−3)	3.3289(−3)	−0.31
20	3.6112(−2)	3.6000(−2)	−0.31	4.2575(−6)	4.3034(−6)	1.08
50	3.6112(−2)	3.5995(−2)	−0.32	1.0236(−14)	1.0672(−14)	4.26

and efficient and makes the successive order of scattering method applicable for optically thick scattering media.

Acknowledgements

This research was supported by the Office of Science (BER), US Department of Energy, Grants DE-FG02-03ER63531, and Northeast Regional Center of the National Institute for Global Environmental Change (NIGEC) under Cooperative Agreement no. DE-FC03-90ER61010. Data were obtained from the Atmospheric Radiation Measurement (ARM) Program sponsored by the US Department of Energy, Office of Energy Research, Office of Health and Environmental Research, Environmental Sciences Division.

References

[1] Min Q-L, Duan M. A successive order of scattering model for solving vector radiative transfer in the atmosphere. JQSRT 2004;87:243–60.
[2] Herman BM, Asous W, Browning SR. Semi-analytic technique to integrate the radiative transfer equation over optical depth. J Atmos Sci 1980;37:1828–38.

[3] Lenoble J. Radiative transfer in scattering and absorbing atmospheres: standard computational procedures. A.Deepak publishing, 1985. p. 47.
[4] Tomas G, Stamnes K. Radiative transfer in the atmosphere and ocean. Cambridge: Cambridge University Press; 2002. p. 296–302.
[5] Stamnes K, Tsay SC, et al. Numerically stable algorithm for discrete ordinate method radiative transfer in multiple scattering and emitting layered media. Appl Opt 1998;27:2502–9.